Supporting Information

Carbon Monoxide in Controlling the Surface Formation of Group VIII Metal Nanoparticles

Sang Youp Hwang, [+],[†] Mingzhen Zhang,[+],[†] Changlin Zhang, [†] Buyong Ma,[‡] Jie Zheng,[†] and

Zhenmeng Peng*,[†]

[†]Department of Chemical and Biomolecular Engineering, University of Akron, Whitby Hall 211,

Akron, OH 44325, United States

[‡]Cancer and Inflammation Program, National Cancer Institute, Frederick, Maryland 21702,

United States

[+]Equal contribution

*Corresponding author. E-mail: zpeng@uakron.edu (Z. P.). Office: (330) 972-5810

EXPERIMENTAL SECTION

Materials. Nickel acetylacetonate (Ni(acac)$_2$, 95%), ruthenium acetylacetonate (Ru(acac)$_3$, 97%), rhodium acetylacetonate (Rh(acac)$_3$, 97%), iridium acetylacetonate (Ir(acac)$_3$, 97%), palladium acetylacetonate (Pd(acac)$_2$, 99%), platinum acetylacetonate (Pt(acac)$_2$, 97%), oleylamine (OAm, technical grade 70%), oleic acid (OA, technical grade 90%), and polyvinylpyrrolidone (PVP, M$_W$=360,000) were purchased from Sigma-Aldrich. Acetone (C$_3$H$_6$O, 99.8%), toluene (C$_7$H$_8$, 99.9%), and ethanol (EtOH, 95.3%) were purchased from Fisher Scientific. Ethylene glycol (EG, semi grade) was from VWR. Amorphous carbon (Vulcan® XC-72R, Cabot) and silica (SiO$_2$, Sigma-Aldrich) were used as support materials. Carbon monoxide (CO, 99.5%) and argon (Ar, 99.999%) gases were from Praxair. A gas filter (Labclear®) was equipped to remove residual metal carbonyls in carbon monoxide gas before use.

Synthesis of Shaped GVIIIM Nanoparticles. All synthetic experiments for making shaped nanoparticles were conducted under continuous magnetic stirring and under CO atmosphere using a standard Schlenk line.

Icosahedral Ni. Ni(acac)$_2$ (20 mg) was dissolved in OAm (8 mL) and OA (2 mL) in a 25-mL three-neck flask. The resulting solution was firstly saturated by dissolved CO through bubbling the gas into the solution for about 30 min. The solution was then gradually heated to 210 °C using oil bath and kept at the temperature for 1 h. The product was precipitated out by washing with ethanol, followed by centrifugation at 4000 rpm for 1 min. The precipitate was dispersed in toluene for characterization.

Decahedral Ru. Ru(acac)$_3$ (40 mg) and PVP (6 mg) were dissolved in EG (10 mL) in a 25-mL three-neck flask, which was then saturated by dissolved CO by bubbling the gas into the solution. The reaction mixture was gradually heated to the refluxing temperature using oil bath

and reacted at the temperature for 1 h. The produced particles were washed with ethanol and precipitated by centrifugation at 6000 rpm for 5 min, and were dispersed in ethanol for characterization.

Decahedral Ir. Ir(acac)$_3$ (25 mg) was dissolved in OAm (5 mL) in a 25-mL three-neck flask, which was then saturated by dissolved CO. The solution was gradually heated to 290 °C using heating mantle and was kept at the temperature for 2 h. The synthesized Ir nanoparticles were washed with ethanol and precipitated by centrifugation at 4000 rpm for 1 min, and were dispersed in toluene for characterization.

Tetrahedral Rh. Rh(acac)$_3$ (20 mg) was dissolved in OAm (10 mL) in a 25-mL three-neck flask, which was then saturated by dissolved CO. The solution was gradually heated to 250 °C using oil bath and kept at the temperature for 1 h. The product was washed with ethanol and precipitated by centrifugation at 4000 rpm for 1 min, and was dispersed in toluene for characterization.

Concaved-tetrahedral and plate-like Pd. Pd(acac)$_2$ (20 mg) was dissolved in OAm (8 mL) and OA (2 mL) in a 25-mL three-neck flask, which was then saturated by dissolved CO. The solution was gradually heated to 120 °C using oil bath and kept at the temperature for 1 h. The product was washed with ethanol and precipitated by centrifugation at 4000 rpm for 1 min, and was dispersed in toluene for characterization.

Cubic Pt. Pt(acac)$_2$ (20 mg) was dissolved in OAm (8 mL) and OA (2 mL) in a 25-mL three-neck flask, which was then saturated by dissolved CO. The solution was gradually heated to 200 °C using oil bath and kept at the temperature for 1 h. The product was washed with ethanol and precipitated by centrifugation at 2000 rpm for 1 min. The washed particles were dispersed in toluene for characterization.

Control experiments.

Synthesis of GVIIIM nanoparticles without CO. The experiments were conducted to investigate the influence of CO on the surface formation of growing GVIIIM particles (M = Ni, Ru, Rh, Pd, Ir, and Pt). All the synthetic parameters for preparing these metal particles were maintained the same as for preparing their shaped counterparts, except that an Ar atmosphere instead of CO was used for the synthesis.

Synthesis of cubic Pt in PVP-EG. $Pt(acac)_2$ (20 mg) and PVP (90 mg) were dissolved in EG (10 mL) in a 25-mL three-neck flask, which was then saturated by dissolved CO. The solution was gradually heated to refluxing temperature using oil bath and kept at the temperature for 1 h. The product was washed with ethanol and precipitated by centrifugation at 6000 rpm for 5 min. The washed particles were dispersed in ethanol for characterization.

Characterizations. The GVIIIM nanoparticles were characterized by taking transmission electron microscopy (TEM) images using a JEOL JEM-1230 microscope with an accelerating voltage of 120 KV. High-resolution TEM (HRTEM) images were taken using a FEI Tecnai G2 F20 microscope operated at 200 KV. The accurate metal loading of Pt/C products was determined by heating the samples at 5 °C/min to 750 °C in a flow of air (60 cm^3/min) to burn off C and measuring weight of residue in a thermal gravimetric instrument (TA Instruments, Model Q50). Powder X-ray Diffraction (PXRD) also were taken using Bruker AXS D8 Discover X-Ray with Cu Kα (λ=1.54 Å).

***In Situ* FTIR Measurements.** In situ Fourier transform infrared spectroscopy (FTIR) experiments were carried out using a Thermo Scientific Nicolet 6700 spectrometer, which is equipped with a liquid nitrogen (LN_2) cooled MCT detector and a diffuse reflectance infrared

Fourier transform (DRIFT) system. Metal precursors, $M(acac)_n$ (n=2 or 3), were put onto a SiO_2 support and transferred into the chamber of a high temperature/high pressure reaction cell (Praying Mantis™, Harrick Scientific Products, Inc.). The reaction cell is equipped with KBr windows, and a K-type thermocouple and a temperature controller. The samples were first flushed with Ar for around 30 min for removal of air and moisture. The gases were then switched to 100/8 sccm CO/H_2. The samples were heated at 5 °C/min to designated temperature and maintained at the temperature for 1 hour. Time-lapsed spectra were collected continuously every one minute by averaging 32 scans taken with 4 cm^{-1} resolution.

DFT Calculations. The CASTEP (Cambridge Sequential Total Energy Package), a leading code for simulation of the property of materials using the density functional theory (DFT), was employed to calculate the adsorption energy (E_{ad}) of CO molecules on different metalsurfaces. The structures were optimized using Perdew-Burke-Ernzerhof function (PBE) based on the generalized gradient approximation (GGA). The ultrasoft pseudopotential was chosen to describe the inner-shell electrons throughout the calculations. No restrictions in symmetry and spin were applied in all the calculations. An energy cutoff of 300 eV, a K-point separation of 0.05 eV/Å, and a SCF (self-consistent filed) convergence tolerance of less than 2.0×10^{-6} eV were applied to obtain the computational precision. The structures of both metal surfaces ((100), (111), and (110) for Ni, Ru, Ir, Rh, Pd, and Pt) and CO molecule were fully optimized before they were put together. The entire structure consisting of both metal surfaces and CO were then optimized to reach the most stable conformation. The E_{ad} was calculated from the following equation:

$$E_{ad} = E_{total} - E_M - E_{CO} \qquad (1)$$

where E_{total}, E_M, and E_{CO} denote the energy of CO-adsorbed metal surface, clean metal surface, and free CO molecule, respectively.
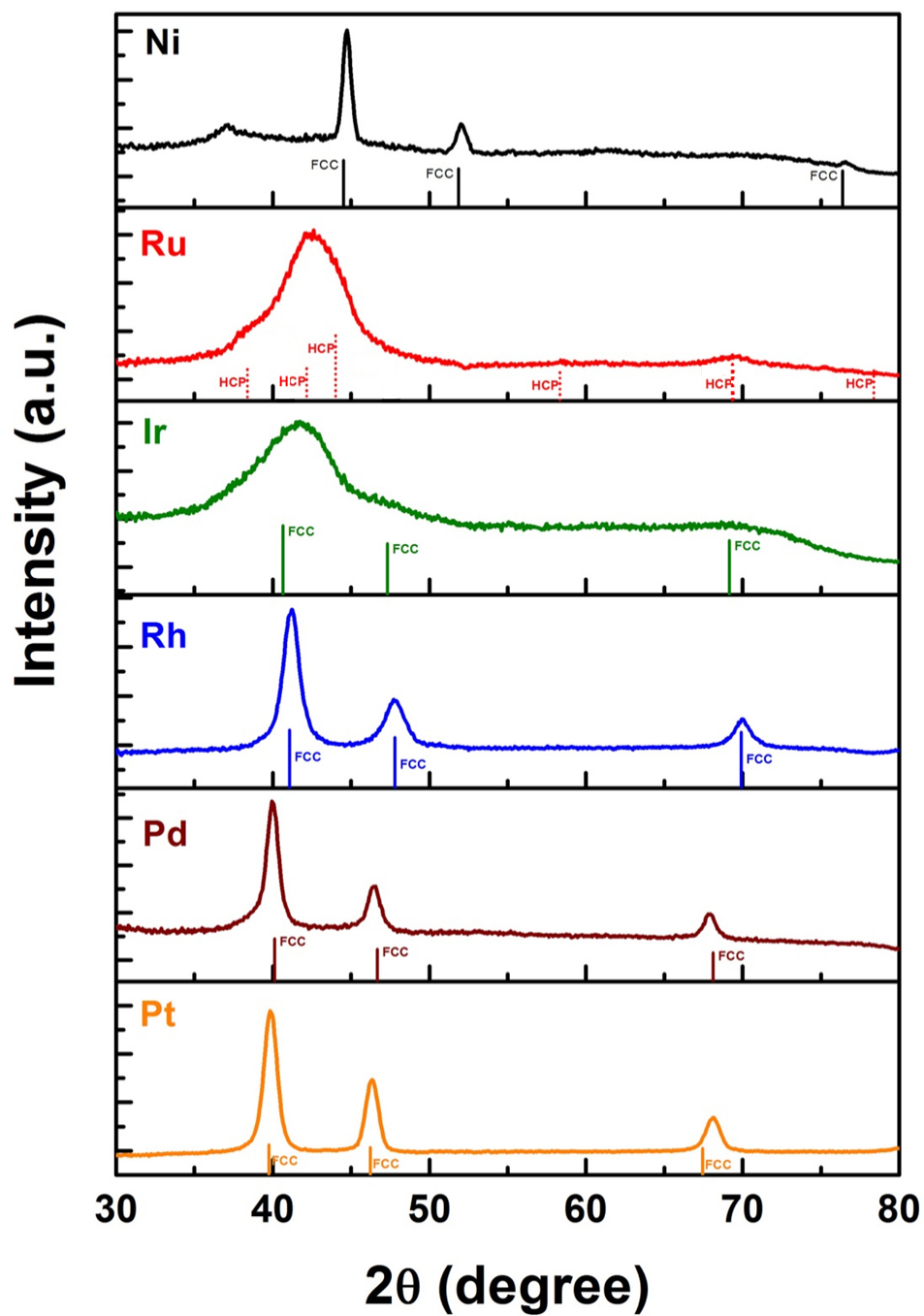
Figure S1. PXRD patterns of as-synthesized icosahedral Ni, decahedral Ru and Ir, tetrahedral Rh, concaved-tetrahedral/plate-like Pd, and cubic Pt nanoparticles.
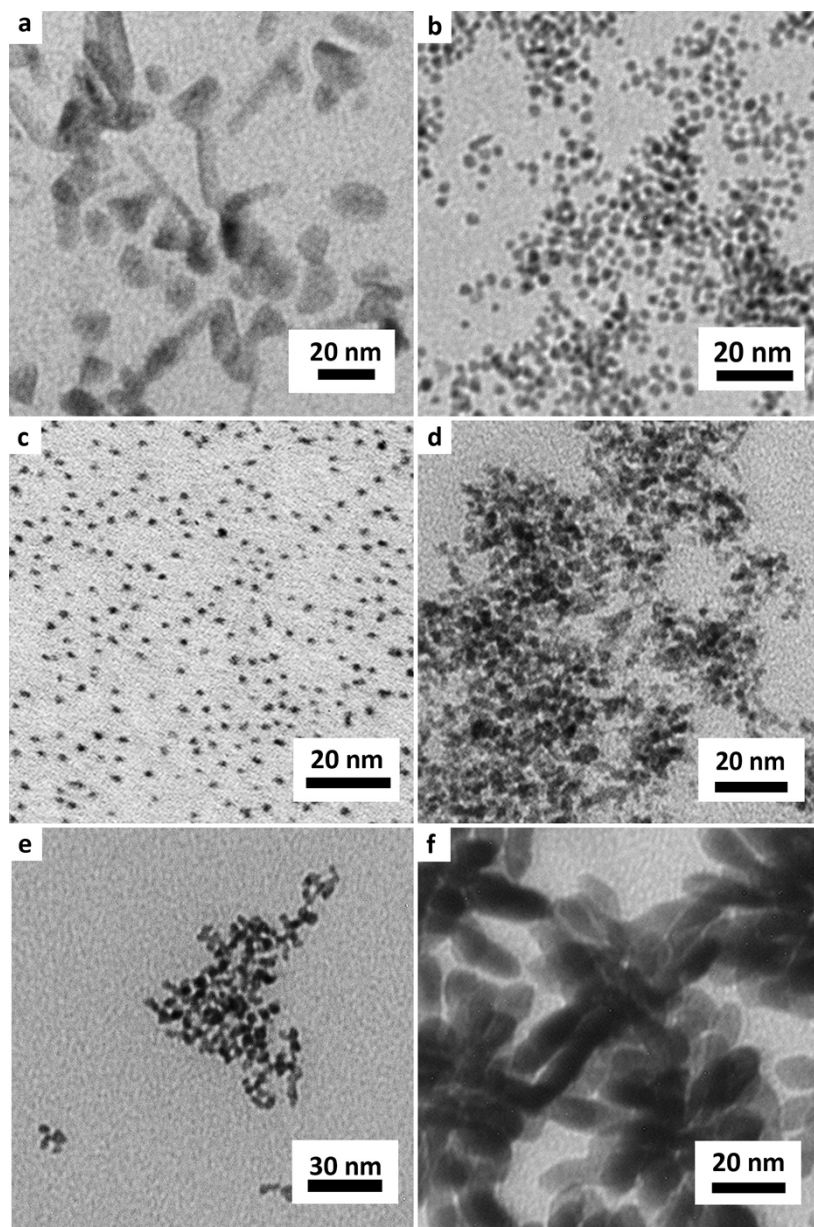
Figure S2. TEM images of (a) Ni, (b) Ru, (c) Ir, (d) Rh, (e) Pd, and (f) Pt nanostructures synthesized in the absence of CO.
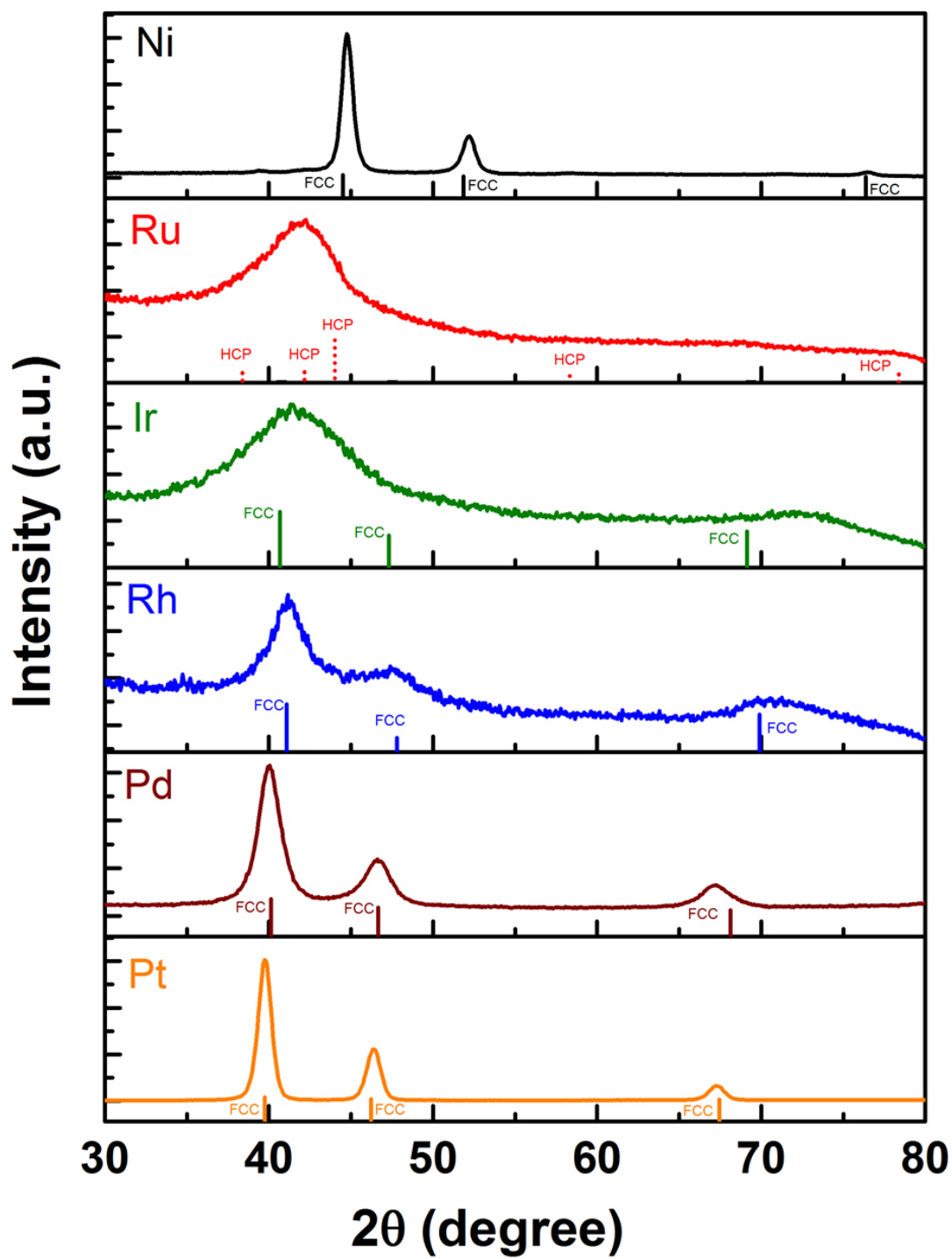
Figure S3. Powder X-ray diffraction (PXRD) patterns of as-synthesized Ni, Ru, Ir, Rh, Pd, and Pt nanoparticles in the absence of CO.
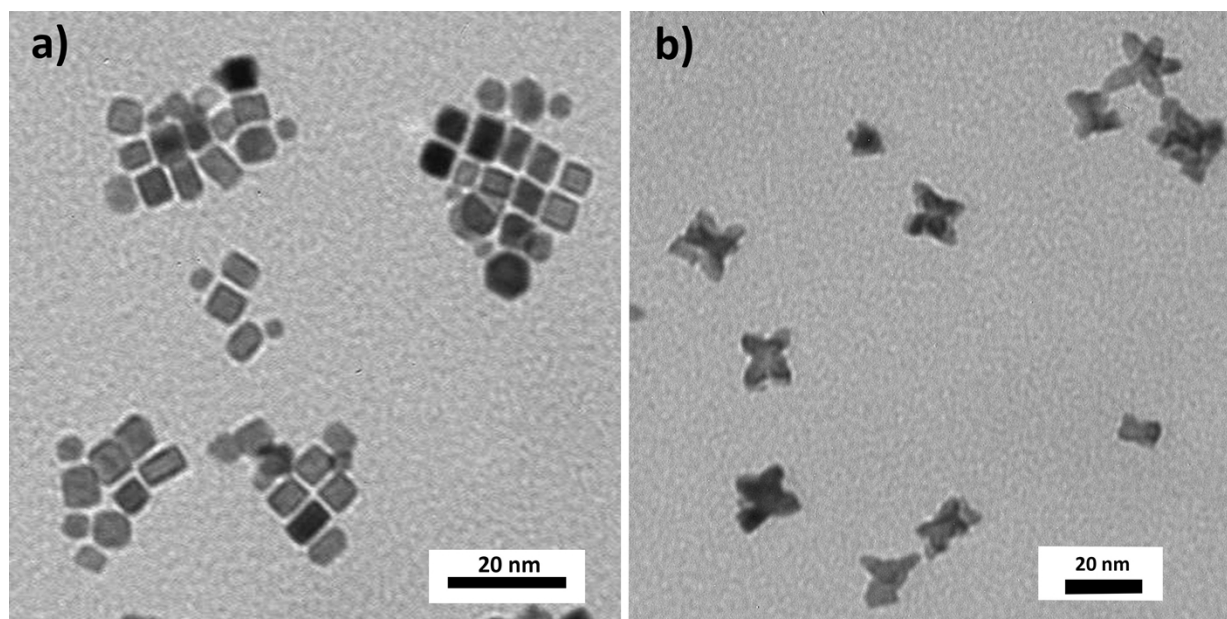
8

Figure S4. TEM images of Pt nanoparticle synthesized using a PVP-EG system (a) in the presence of CO and (b) in the absence of CO.
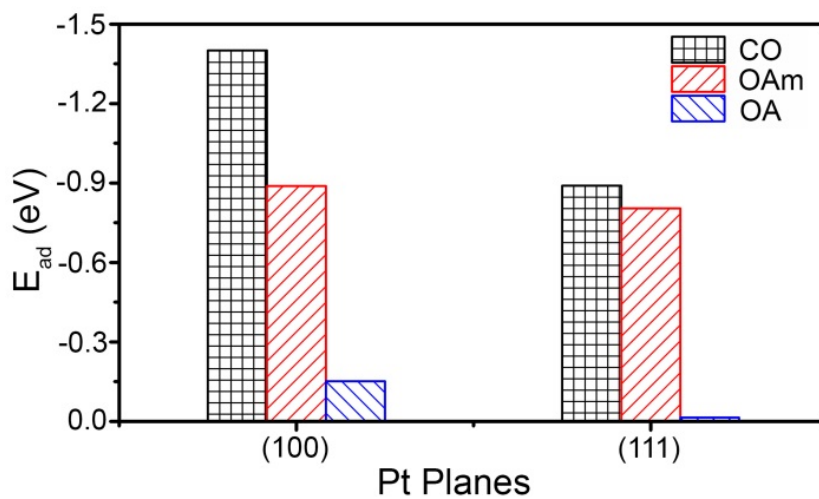

Figure S5. Comparison of DFT-calculated adsorption energy (E_{ad}) of CO, OAm, and OA molecules on different Pt surface planes.
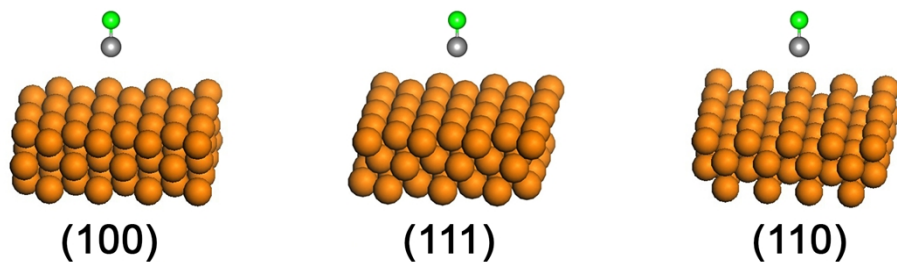
Figure S6. Schematic model sets for DFT calculation of CO adsorption energy on difference surfaces of group VIII metals: green, O; grey, C; and orange, M (M = Ni, Ru, Ir, Rh, Pd, and Pt).
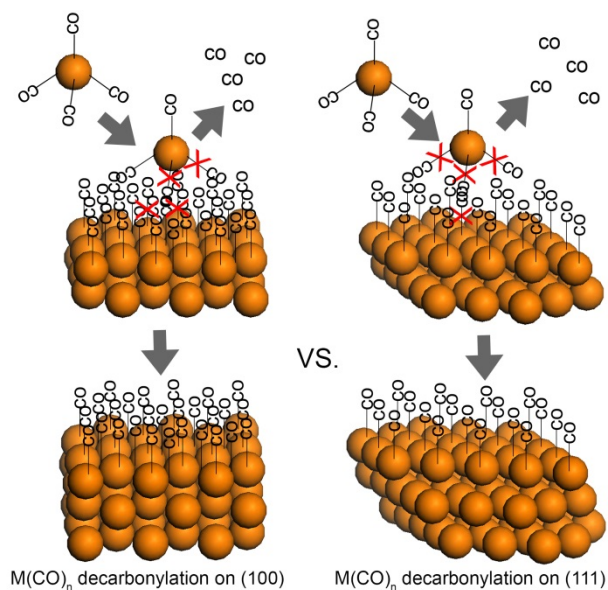

M(CO)$_n$ decarbonylation on (100)   M(CO)$_n$ decarbonylation on (111)

Figure S7. Schematic illustration of the growth of (100) and (111) planes through M(CO)$_n$ decarbonylation on the CO-adsorbed surfaces for metals including Ni, Ru, Ir, and Rh.
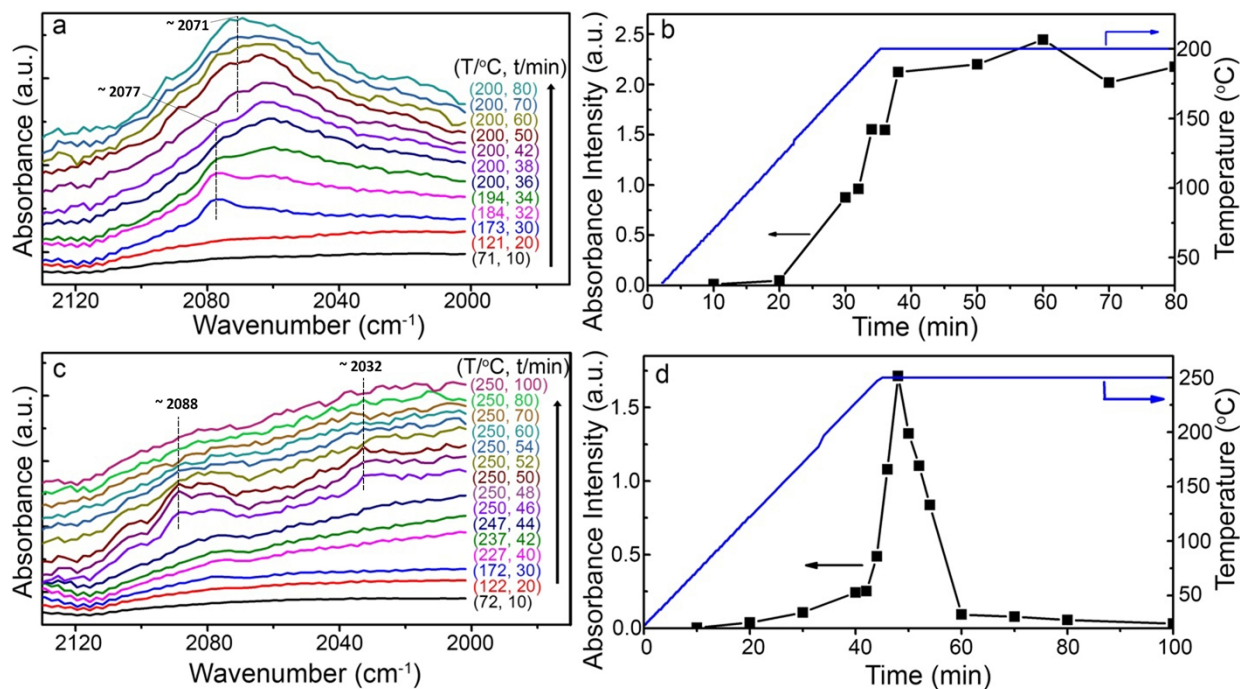
Figure S8. In situ FTIR spectra and changes in CO absorbance intensity during (a, b) Pt(acac)$_2$ and (b) Rh(acac)$_3$ reduction.

Table S1. DFT-calculated CO adsorption energy (E_{ad}) on group VIII metals.

Metal	Surface plane	E_{ad} (eV)		
		A-top adsorption	Bridge adsorption	3-fold adsorption
Ni	(100)	-0.68	**-1.02**	-0.79
	(111)	-0.22	-0.49	**-0.59**
Ru	(100)	-1.23	-1.57	**-1.60**
	(111)	-0.75	-1.02	**-1.07**
Ir	(100)	-1.69	**-1.87**	-1.66
	(111)	**-1.17**	-0.89	-0.86
Rh	(100)	-1.23	**-1.57**	-1.19
	(111)	-0.75	-0.91	**-0.96**
Pd	(100)	-0.83	**-1.27**	-0.87
	(111)	-0.52	-0.80	**-0.90**
	(110)	-1.37	**-1.74**	-0.87
Pt	(100)	-1.13	**-1.40**	-1.13
	(111)	**-0.89**	-0.85	-0.76